Journal Pre-proof

Bayesian brain in tinnitus: Computational modeling of three perceptual phenomena using a modified Hierarchical Gaussian Filter

Suyi Hu, Deborah A. Hall, Frederic Zubler, Raphael Sznitman, Lukas Anschuetz, Marco Caversaccio, Wilhelm Wimmer

PII: S0378-5955(21)00172-6
DOI: https://doi.org/10.1016/j.heares.2021.108338
Reference: HEARES 108338

To appear in: *Hearing Research*

Received date: 22 February 2021
Revised date: 27 May 2021
Accepted date: 17 August 2021

Please cite this article as: Suyi Hu, Deborah A. Hall, Frederic Zubler, Raphael Sznitman, Lukas Anschuetz, Marco Caversaccio, Wilhelm Wimmer, Bayesian brain in tinnitus: Computational modeling of three perceptual phenomena using a modified Hierarchical Gaussian Filter, *Hearing Research* (2021), doi: https://doi.org/10.1016/j.heares.2021.108338

Highlights

- We present a generative computational model for perceptual phenomena in tinnitus subjects based on the Bayesian brain concept.
- The model is able to reproduce the tinnitus phenomena of residual inhibition, residual excitation and the occurrence of tinnitus after sensory deprivation.
- The model can be used to design and optimize behavioral testing paradigms and to guide future tinnitus research.

Graphical Abstract

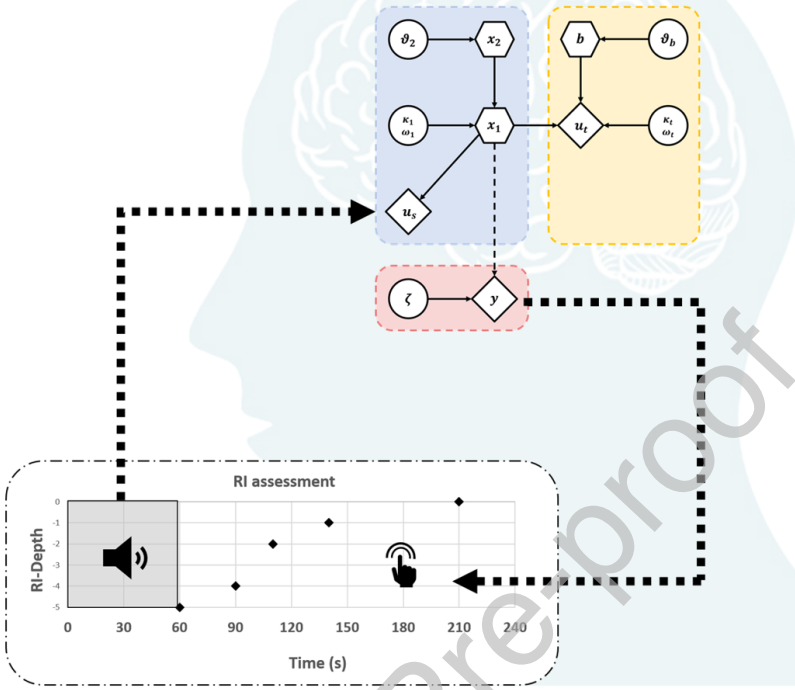

Bayesian brain in tinnitus: Computational modeling of three perceptual phenomena using a modified Hierarchical Gaussian Filter

Suyi Hu[1,2], Deborah A. Hall[3,4], Frederic Zubler[5], Raphael Sznitman[6], Lukas Anschuetz[1], Marco Caversaccio[1,2], Wilhelm Wimmer[1,2*]

August 23, 2021

* Corresponding author

1. Department for Otolaryngology, Head and Neck Surgery, Inselspital, University Hospital Bern, University of Bern, Switzerland.
2. Hearing Research Laboratory, ARTORG Center for Biomedical Engineering Research, University of Bern, Switzerland
3. Hearing Sciences, Division of Clinical Neuroscience, School of Medicine, University of Nottingham, Nottingham, UK
4. Department of Psychology, School of Social Sciences, Heriot-Watt University Malaysia, Putrajaya, Malaysia
5. Department of Neurology, Inselspital, University Hospital Bern, University of Bern, Switzerland.
6. Artificial Intelligence in Medical Imaging, ARTORG Center for Biomedical Engineering Research, University of Bern, Switzerland

Highlights

- We present a generative computational model for perceptual phenomena in tinnitus subjects based on the Bayesian brain concept.
- The model is able to reproduce the tinnitus phenomena of residual inhibition, residual excitation and the occurrence of tinnitus after sensory deprivation.
- The model can be used to design and optimize behavioral testing paradigms and to guide future tinnitus research.

Abstract

Recently, Bayesian brain-based models emerged as a possible composite of existing theories, providing an universal explanation of tinnitus phenomena. Yet, the involvement of multiple synergistic mechanisms complicates the identification of behavioral and physiological evidence. To overcome this, an empirically tested computational model could support the evaluation of theoretical hypotheses by intrinsically encompassing different mechanisms. The aim of this work was to develop a generative computational tinnitus perception model based on the Bayesian brain concept. The behavioral responses of 46 tinnitus subjects who underwent ten consecutive residual inhibition assessments were used for model fitting. Our model was able to replicate the behavioral responses during residual inhibition in our cohort (median linear correlation coefficient of 0.79). Using the same model, we simulated two additional tinnitus phenomena: residual excitation and occurrence of tinnitus in non-tinnitus subjects after sensory deprivation. In the simulations, the trajectories of the model were consistent with previously obtained behavioral and physiological observations. Our work introduces generative computational modeling to the research field of tinnitus. It has the potential to quantitatively link experimental observations to theoretical hypotheses and to support the search for neural signatures of tinnitus by finding correlates between the latent variables of the model and measured physiological data.

Keywords

Generative model, Computational modelling, Residual inhibition, Residual excitation, tinnitus model.

1 Introduction

Subjective tinnitus is a conscious auditory perception in the absence of external or internal sound sources. Up to 30% of the population experience bothersome tinnitus, but this depends on the methodology and age group surveyed (McCormack et al., 2016). Evidence of abnormal neural activity along the auditory pathway up to the auditory cortex and other high-level networks suggests that both peripheral and central systems are involved in the development and maintenance of tinnitus (Carpenter-Thompson et al., 2014, De Ridder et al., 2011, Eggermont and Roberts, 2004, Jastreboff, 1990, Norena, 2011, Silchenko et al., 2013, Xiong et al., 2019).

A variety of models have been developed to explain tinnitus and related sound-triggered phenomena (De Ridder et al., 2014c, 2015, Norena and Eggermont, 2003, Noreña and Eggermont, 2006, Rauschecker et al., 2015, Roberts et al., 2013, Schaette and McAlpine, 2011, Seki and Eggermont, 2003, Zeng, 2013). Recently, modelling approaches based on the Bayesian brain, a fundamental framework for predictive processes, have gained attention in tinnitus research. Under the Bayesian brain perspective, perception is considered as the active inference of environmental states under uncertainty based on internal representations of the brain (Clark, 2013, Friston, 2010, Knill and Pouget, 2004). This notion has been applied in predictive coding (Friston, 2010, Rao and Ballard, 1999) and hierarchical Bayesian inference, namely the Hierarchical Gaussian Filter (HGF) (Mathys et al., 2011, 2014), which involves the inclusion of hierarchical predictions of sensory input into the brain. At each layer of the hierarchically structured sensory systems, bottom-up signals (likelihood) from the layer below are compared with the top-down prediction (prior) from the layer above. Their deviations are denoted as prediction errors (PEs) and

are passed to the higher layers to update the predictions with the aim of minimizing the PEs. The magnitude of the PEs is calculated based on the proportion of the confidence levels (precision) of the input and the prediction. Bayesian tinnitus theories assume that tinnitus is a compensatory process to minimize elevated PEs caused either by bottom-up excitatory inputs, false top-down inhibitory predictions, or a combination of both (De Ridder et al., 2014a,b, Hullfish et al., 2018, 2019a, Kumar et al., 2014, Lee et al., 2017, Sedley et al., 2016a, 2019, Vanneste and De Ridder, 2016). Sedley et al. (2016a) proposed a Bayesian brain model in which tinnitus can be synergistically triggered by neurophysiological, hormonal and neurochemical factors. Each of these factors can influence the precision of the bottom-up signal, i.e. the tinnitus precursor, to the auditory cortex. Normally, the top-down default prediction (i.e. the prediction in the absence of external stimuli or 'silence') prevents the auditory perception from tending towards the tinnitus precursor and ignores it as irrelevant noise. However, a sufficiently high precision of the tinnitus precursor leads to a lower degree of confidence in the default prediction - resulting in a deviation from the default perception of "silence". Ultimately, sufficiently long tinnitus chronicity can lead to the formation of a new default prediction (from 'silence to 'tinnitus') that maintains the persistence of the tinnitus.

The Bayesian brain concept can provide explanations for several phenomena observed in tinnitus patients, including residual inhibition (RI) and residual excitation (RE). RI and RE denote the transient suppression or amplification of tinnitus loudness perception after exposure to an acoustic stimulus. A detailed understanding, in particular of RI, is of central importance, as it could be applied to temporarily modulate tinnitus for management and relief in suffering patients (Fournier et al.,

2018, Hu et al., 2021). Moreover, RI enables to investigate tinnitus characteristics using behavioral test paradigms. However, there exists a paradox of neuronal activity in the auditory cortex during RI and RE. RI has been hypothesized to be the consequence of a temporary reduction of successive spontaneous firing and neuronal synchronicity that occur in response to peripheral lesions (Galazyuk et al., 2017, Roberts et al., 2008). Neural imaging studies reported a reduction in low frequency (i.e. delta/theta bands) and high frequency (i.e. gamma band) oscillations in the auditory cortex during RI (Adjamian et al., 2012, Kahlbrock and Weisz, 2008, Sedley et al., 2012, 2015). During RE, however, contrary to the expected increase of oscillations, a decrease of gamma oscillation was observed (Sedley et al., 2012). Magnetoencephalography data collected from patients with tinnitus showed predominantly gamma power positively correlates with tinnitus intensity in those experiencing RI, but the opposite relationship in those experiencing RE (Norena, 2011). This suggests that auditory cortical gamma oscillations suppress, rather than cause, the perception of tinnitus. Applying the Bayesian brain concept, both suppression (RI) and enhancement (RE) of tinnitus can be explained as transient modulation processes of the tinnitus precursor and the default prediction. In both phenomena, the process aims at minimizing the prediction error caused by the acoustic stimulation and manifests itself in a reduction of gamma oscillations.

Although the Bayesian brain approach is promising, the lack of possibilities to link the concepts to observable behavioral or physiological data limits further analysis. To overcome this limitation, generative computational models were proposed in various areas of psychological research. In the related field of auditory hallucinations, studies demonstrated that patients with strong priors (prediction) are more likely to experience hallucinations (Cassidy et al., 2018, Corlett et al.,

2019) and that patients with hallucinations are less likely to update their prior beliefs with new sensory input (Powers et al., 2017). Computational modelling of tinnitus was applied in previous studies (Chrostowski et al., 2011, Gault et al., 2020, Parra and Pearlmutter, 2007, Schaette and Kempter, 2006, 2009, 2012). To evaluate whether these concepts could be advanced, we aimed to develop a generative computational tinnitus model based on the Bayesian brain concept. Such a tinnitus model could be of scientific and clinical importance for several reasons. First, it would enable the quantitative inference of observable data from proposed neurophysiological mechanisms. Second, differences in model parameters could be used for a refined sub-typing of tinnitus, to identify pathophysiological mechanisms and potentially provide a personalized treatment based on behavioral measurements (Stephan et al., 2015). Third, generative computational models could be applied to generate sub-type-specific synthetic data as a basis to design and assess hypotheses of behavioral studies. Fourth, the individual parameter values for each subject address the heterogeneity across tinnitus patients allowing patient tailored treatment in the future, for instance, in combination with neuro-feedback that demonstrated promising results (Güntensperger et al., 2017). We hypothesized that a Bayesian brain-based approach can be used to reproduce RI behavior in tinnitus subjects by introducing a novel generative HGF-based model, the Tinnitus Hierarchical Gaussian Filter (tHGF). The model was tested with behavioral data of tinnitus subjects collected during RI assessment. Since the Bayesian brain concept is also able to explain the phenomena of residual excitation and the occurrence of tinnitus after temporary sensory deprivation (e.g. by using ear plugs), the applicability of the model to generate such phenomena was evaluated.

2 Materials and Methods

2.1 Tinnitus Hierarchical Gaussian Filter (tHGF)

Our computational model is based on the HGF, which applies variational Bayes to infer an individual's belief and uncertainty of hidden environmental states from sensory inputs (Mathys et al., 2011, 2014). The hidden states evolve over time as a hierarchy of coupled Gaussian random walks. At each level of the HGF, the volatility over the hidden states is dynamically estimated by the states of the next higher level. We adopted the HGF in our extended tinnitus model (tHGF) by assessing the continuous updating of subjects' beliefs in tinnitus perception in response to acoustic stimulation. In addition, our model applies the Bayesian approach proposed by Sedley et al. (2016a), in which the posterior distribution represents the auditory perception and is proportionally depending on the sensory evidence (likelihood) and the brain's predictions (prior distributions). These distributions are Gaussian, with the mean representing the auditory intensity (dB SL) and the inverse variance the precision of the perception. According to Sedley et al. (2016a), the likelihood distribution reflects the spontaneous activity along the auditory pathway to the auditory cortex and is denoted as tinnitus precursor. In non-tinnitus subjects, the influence of the tinnitus precursor is eliminated by the prior distribution (the default prediction) with "silence" as the mean value (defined at 0 dB SL) and a dominant precision. Tinnitus occurs either when the mean value of the default prediction is displaced from 0 dB SL or when the precision of the tinnitus precursor increases significantly, which leads to a updated posterior distribution (i.e. auditory perception).

In the tHGF, we combine the approaches of the HGF and the Bayesian theory

proposed by Sedley et al. (2016a). A graphical representation of the tHGF is shown in Figure 1. The trajectories of the hidden environmental states (including the auditory perception) are derived from the perceptual model (blue and yellow areas in Figure 1), while the response model (red area in Figure 1) translates them into the behavioral responses of the subjects. The distributions of the hidden states, i.e., their mean and precision, are continuously updated according to the acoustic stimulation (u_s; model input) leading to transiently modulated auditory perception and consequently behavioral responses (y; model output). In our model, the sensory evidence is assumed to be formed as a joint distribution of the tinnitus precursor (u_t; a fitted model variable) and external acoustic stimuli (u_s; model input). The probability distribution of the external acoustic stimulation can be represented by a Gaussian distribution with mean at the stimulation level (in dB SL) and a high precision. In the absence of stimulation, a level of 0 dB SL and a low precision are used as model input. The probability distribution of the tinnitus precursor is approximated as consisting of a time-invariant mean representing a subject-specific auditory intensity and a time-varying precision updated based on its higher level. This model offers the possibility to choose between fixed parameters or to fit all time-invariant constants (i.e. circles in Figure 1), the prior distribution (i.e., the initial values for mean and variance before any external stimulation, i.e., the steady state) of the time-varying states (i.e., hexagons in Figure 1), and the the tinnitus precursor (i.e., the time-invariant mean value and the prior variance of u_t). The details of the models used for the evaluation (i.e. which parameters were selected as fixed or tuned by model fitting) are presented in the section 2.3.

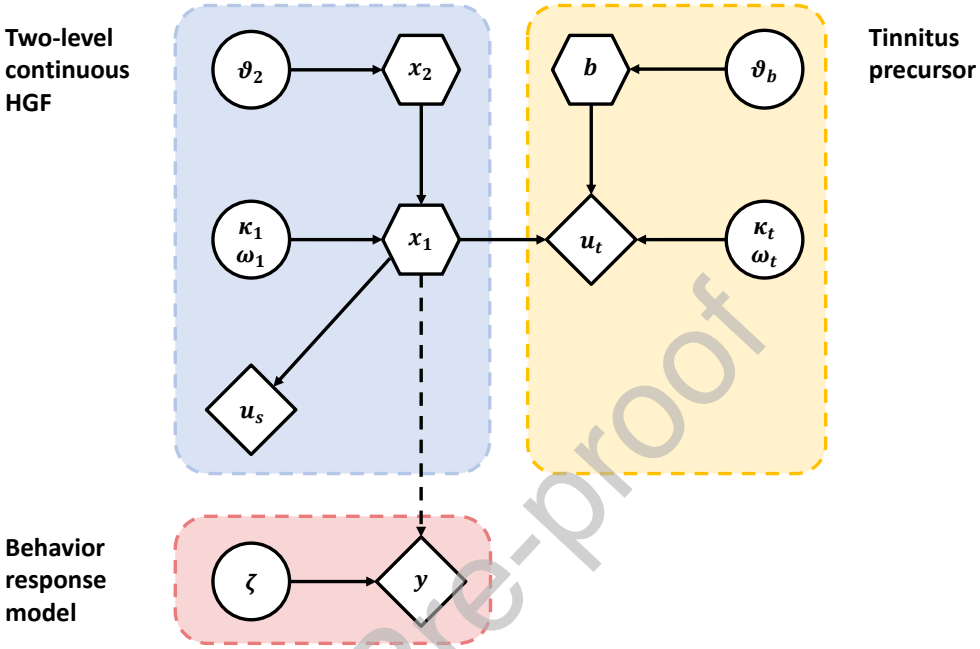

Figure 1: Graphical representation of the Tinnitus Hierarchical Gaussian Filter (tHGF). Diamonds and hexagons represent quantities that change in time, while hexagons additionally depend in a Markovian fashion on the previous state in time. Parameters in circles are time-invariant constants. A two-level continuous HGF was used as the basis (blue area).The acoustic stimulation, i.e. u_s, is used as a model input (sensory input). The first level x_1 estimates the auditory perception of the subjects, while its certainty is controlled by the second level x_2 with the coupling strength κ_1 and the logarithmic volatility ω_1. The estimation of auditory perception additionally depends on a second input, the tinnitus precursor u_t (yellow area). The certainty of the tinnitus precursor is determined by the higher level b. The volatilities of the second levels (i.e. x_2 and b) are determined by the time-invariant parameters ϑ_2 and ϑ_b. The behavioral response y (model output; red area) depends on the inferred value of x_1, indicated as a dashed line.

2.1.1 Perceptual Model

The perceptual model in the tHGF is based on a two-level continuous HGF (Mathys et al., 2014) for estimating the behavioral responses $y^{(k)}$ of the subjects (model output or decisions), where k represents a time index. We extend the model by adding the components regarding the tinnitus precursor. The lower level $x_1^{(k)}$ represents the hidden state about the intensity of an auditory perception (in dB SL). The precision, i.e. how certain a subject is about the perception, is determined by the state of the second level $x_2^{(k)}$. In the following description, the expected values of posterior beliefs about the states at a certain level i are called $\mu_i^{(k)}$, while $\hat{\mu}_i{}^{(k)}$ is used to denote predictions before new inputs are observed.

The sensory input in the tHGF is composed of the acoustic stimulation $u_s^{(k)}$ (model input) and the tinnitus precursor $u_t^{(k)}$ to infer the hidden state $x_1^{(k)}$, with the variances (i.e. the inverse of the sensory precision) $\left(\pi_s^{(k)}\right)^{-1}$ and $\left(\pi_t^{(k)}\right)^{-1}$, respectively. The sensory precision π_s is lower in the absence of stimulation (denoted as Π_0):

$$u_s^{(k)} \sim \mathcal{N}\left(x_1^{(k)}, \left(\pi_s^{(k)}\right)^{-1}\right), \tag{1}$$

$$u_t^{(k)} \sim \mathcal{N}\left(x_1^{(k)}, \left(\pi_t^{(k)}\right)^{-1}\right), \tag{2}$$

$$\pi_s^{(k)} = \begin{cases} \Pi_0 & \text{if } x_1^{(k)} = 0 \text{ dB SL} \\ \Pi_s & \text{if } x_1^{(k)} = \text{stimulus level (in dB SL)} \quad \text{with } \Pi_s \gg \Pi_0. \end{cases} \tag{3}$$

The tinnitus precursor $u_t^{(k)}$ is defined as spontaneous activity along the auditory pathway (Sedley et al., 2016a). In our model, $u_t^{(k)}$ is approximated as a time-

invariant and subject-specific auditory intensity (referred to as U_t) above tinnitus perception level. The updating equation for the posterior belief on auditory perception $\mu_1^{(k)}$ after receiving sensory input is:

$$\mu_1^{(k)} = \hat{\mu_1}^{(k)} + \frac{\hat{\pi}_s^{(k)}}{\pi_1^{(k)}} \cdot \delta_s^{(k)} + \frac{\hat{\pi}_t^{(k)}}{\pi_1^{(k)}} \cdot \delta_t^{(k)}, \tag{4}$$

with the prediction errors

$$\delta_s^{(k)} = u_s^{(k)} - \hat{\mu_1}^{(k)}, \tag{5}$$

$$\delta_t^{(k)} = U_t - \hat{\mu_1}^{(k)}. \tag{6}$$

In addition, we have

$$\hat{\mu_1}^{(k)} = \mu_1^{(k-1)}, \tag{7}$$

$$\pi_1^{(k)} = \hat{\pi}_1^{(k)} + \hat{\pi}_s^{(k)} + \hat{\pi}_t^{(k)}, \tag{8}$$

$$\hat{\pi}_1^{(k)} = \frac{1}{\left(\pi_1^{(k-1)}\right)^{-1} + \exp\left(\kappa_1 \cdot \mu_2^{(k-1)} + \omega_1\right)}. \tag{9}$$

The precision of the first level is determined by the belief about the state of the higher level $x_2^{(k)}$ (i.e., $\hat{\mu}_2^{(k)}$), which is updated via the prediction error $\delta_1^{(k)}$, weighted by the precision:

$$\mu_2^{(k)} = \hat{\mu}_2^{(k)} + \frac{1}{2} \cdot \frac{1}{\pi_2^{(k)}} \cdot \kappa_1 \cdot w_1^{(k)} \cdot \delta_1^{(k)} \text{ and} \tag{10}$$

$$w_1^{(k)} = \exp\left(\kappa_1 \cdot \mu_2^{(k-1)} + \omega_1\right) \cdot \hat{\pi}_1^{(k)}, \tag{11}$$

with

$$\delta_1^{(k)} = \left(\frac{1}{\pi_1^{(k)}} + \left(\mu_1^{(k)} - \hat{\mu_1}^{(k)}\right)^2\right) \cdot \hat{\pi}_1^{(k)} - 1, \tag{12}$$

$$\pi_2^{(k)} = \hat{\pi}_2^{(k)} + \frac{1}{2} \cdot \kappa_1^2 \cdot w_1^{(k)} \cdot \left(w_1^{(k)} + (2 \cdot w_1^{(k)} - 1) \cdot \delta_b^{(k)}\right), \tag{13}$$

$$\hat{\pi}_2^{(k)} = \frac{1}{\left(\pi_2^{(k-1)}\right)^{-1} + \vartheta_2}. \tag{14}$$

We introduce an AR(1) auto-regressive process to the state $x_2^{(k)}$, pushing $x_2^{(k)}$ towards a restriction parameter m_2 with a change rate of ϕ_2, to prevent the occurrence of infinite precision:

$$\hat{\mu}_2^{(k)} = \mu_2^{(k-1)} + \phi_2 \cdot \left(m_2 - \mu_2^{(k-1)}\right) \tag{15}$$

In our model, the precision of the tinnitus precursor $\pi_t^{(k)}$ is determined by the second level $b^{(k)}$ (with a fixed variance ϑ_b), that is modulated proportionally to the deviations between the posterior perception $\mu_1^{(k)}$ and the tinnitus precursor U_t (i.e. the prediction error $\delta_b^{(k)}$). Greater deviations lead to an increased uncertainty (i.e. decrease of the precision) of the tinnitus precursor.

$$\hat{\pi}_t^{(k)} = \exp\left(-\left(\kappa_t \cdot \mu_b^{(k)} + \omega_t\right)\right), \tag{16}$$

$$\mu_b^{(k)} = \hat{\mu}_b^{(k)} + \frac{1}{2} \cdot \left(\pi_b^{(k)}\right)^{-1} \cdot \kappa_t \cdot \delta_b^{(k)}, \tag{17}$$

$$\delta_b^{(k)} = \left(\frac{1}{\pi_1^{(k)}} + \left(\mu_1^{(k)} - U_t\right)^2\right) \cdot \hat{\pi}_t^{(k)} - 1. \tag{18}$$

Same as for $x_2^{(k)}$, an AR(1) auto-regressive process was implemented to prevent infinite precision of tinnitus precursor in the second level $b^{(k)}$:

$$\hat{\mu}_b = \mu_b^{(k-1)} + \phi_b \cdot \left(m_b - \mu_b^{(k-1)}\right). \tag{19}$$

For the precision of the second level of the tinnitus precursor $b^{(k)}$ we have

$$\pi_b^{(k)} = \hat{\pi}_b^{(k)} + \frac{1}{2} \cdot \kappa_t^2 \cdot \left(1 + \delta_b^{(k)}\right), \tag{20}$$

$$\hat{\pi}_b^{(k)} = \frac{1}{\left(\pi_b^{(k-1)}\right)^{-1} + \vartheta_b}. \tag{21}$$

The coupling factors (κ_1, κ_t) and the volatilities (ω_1, ω_t) control the dependence of the precision of the first levels on the states of the second levels. The updating of the precision decreases as κ_1 or κ_t are reduced, corresponding to a stronger belief in priors.

2.1.2 Response Model

A Gaussian noise model is used to map the subjects' belief in perception $\mu_1^{(k)}$ to their behavioral responses $y^{(k)}$:

$$P(y^{(k)} \mid \mu_1^{(k)}) = \mathcal{N}(\mu_1^{(k)}, \zeta), \tag{22}$$

where the variance ζ represents the noise in the measurement, neural processing, and additional noise sources not covered by the perceptual model.

2.2 Behavioral data

2.2.1 Data Collection

The behavioral data used for modeling were collected in a study investigating the association between RI and neural activity in subjects with tinnitus. The study was approved by the local institutional review board (reference number: KEK-BE 2017-02037). A detailed description of the measurement setup and procedures for audiometric and tinnitometric assessment is provided in the published study protocol (Hu et al., 2019). The behavioral task consisted of ten consecutive trials. In each trial, a personalized narrow-band noise stimulus was presented bilaterally to the subjects for 60 seconds to cause RI (Hu et al., 2019). The subjects were asked to rate the RI depth on an 11-point Likert scale (range: -5 to 5; -5 complete suppression, 0 no change, +5 gain) immediately after stimulus end. The next trial was started after the subjects indicated that their tinnitus had reached the initial tinnitus loudness level (i.e. by indicating 0). During the experiments, the indicated RI depth and time of response (referred to as "RI time") were recorded (Figure 2 (a)). For the model, we used data from 46 tinnitus subjects that were susceptible to substantial RI, i.e. subjects who achieved an averaged maximum RI depth of -5 or -4 over the 10 trials, corresponding to a complete or almost complete suppression of tinnitus (Hu et al., 2021). The demographic details of the subjects can be found

in Supplementary Table S1.

2.2.2 Data Preprocessing

For an appropriate model output, the behavioral responses of discrete-time categorical variables were mapped to continuous trajectories of tinnitus loudness in dB sensation level (SL). For this purpose, the individual tinnitus loudness (in dB SL) determined from tinnitometry (Hu et al., 2019) was used as the reference level, corresponding to an RI depth of 0. The RI depth of -5 was defined as a tinnitus level of 0 dB SL (complete suppression). A sigmoid function was fitted to the discrete RI depth responses of the ten trials to generate a single continuous behavioral response at a sampling rate of 10 Hz, corresponding to a sampling step of 0.1 second (Figure 2 (b)). The found continuous tinnitus loudness trajectory was replicated ten times and applied as the model output based on the robustness of the short-term repeatabilty of the subjects' responses during RI (Hu et al., 2021). During stimulation, the behavioral response to acoustic perception of the subjects was defined to be identical to the stimulus level (Figure 2 (c)). In addition, eight-minute long baseline periods with the initial tinnitus loudness level prior to and at the end of the 10 trials were added, assuming that the tinnitus loudness of all subjects remained in a steady state before and after the behavioral task (Figure 2 (c)).

2.3 Model Fitting and Model Selection

To evaluate the performance of tHGF, we compared it with three other perceptual models. i) Model 1 is a conventional two-level continuous HGF (Mathys et al.,

2014). It was used as a baseline for performance evaluation. ii) Model 2 is a simplified version of tHGF to investigate the influence of the tinnitus precursor. It was specified such that the precision of the tinnitus precursor is assumed to be zero (i.e. without tinnitus precursor; $\pi_t^{(k)} = 0$). iii) In model 3, we included a fixed tinnitus precursor (i.e. with a time-invariant precision: $\pi_t^{(k)} = \Pi_t$). iv) Model 4 represents the complete tHGF and enables the reduction in the sensory precision of the tinnitus precursor after stimulation, which leads to a stronger belief in perceiving silence. We combined each perceptual model with two different response models, with either a fixed or a subject-fit noise parameter ζ.

All models were fitted with the collected behavioral data from 46 subjects. For each model parameter, its prior distribution, i.e. the prior mean and prior variance, was defined before model fitting. In all tested models, it was assumed that the tinnitus perception of the subject remained constant before the behavioral task. Therefore, the mean value of the prior distribution for perception $\mu_1^{(0)}$ was fixed to the subject specific tinnitus intensity, while the mean values of the prior distributions of other states, i.e. $\mu_2^{(0)}$ and $\mu_b^{(0)}$, were set to a neutral value of zero. Additionally, the prior distributions were determined for the model parameters to ensure the constant trajectories of the states and their precision before the behavioral task (steady-state; $\mu_i^{(k)} \stackrel{!}{=} \mu_i^{(k-1)}$ and $\pi_i^{(k)} \stackrel{!}{=} \pi_i^{(k-1)}$). An overview of the parameter settings (i.e., which parameter was set to be fixed or subject to fitting) of 8 models (4 perceptual models times 2 response models) and their prior distributions are presented in Table 1. A parameter was defined as fixed if an infinite prior precision (i.e. a prior variance of zero) was used. Parameters with a non-zero prior variance, including the tinnitus precursor, were fitted.

For parameter estimation, maximum-a-posteriori (MAP) was applied using the

Table 1: Overview of the model parameter settings

Model Input/Output	Parameter	Description	Parameter setting (prior mean; prior variance) Model 1	Model 2	Model 3	Model 4
Sensory Stimulation	u_s	Stimulation level (dB SL)	Subject-specific stimulation level (dB SL)			
	Π_s	Precision with stimulation	Π_0 ; 0	1 ; 4^2	$15 \cdot \Pi_0$; 4^2	
	Π_0	Precision without stimulation	0.1 ; 4^2		$\pi_t^{(0)}\left(\frac{\mu_t^{(0)}}{\mu_1^{(0)}} - 1\right)$; 0	
Responses	y	Auditory perception (dB SL)				
Perceptual Model			Model 1	Model 2	Model 3	Model 4
Perception	$\mu_1^{(0)}$	Initial mean of inferred perception	Subject-specific tinnitus level (dB SL) ; 0			
	$\sigma_1^{(0)}$	Initial variance of μ_1	1 ; 4^2		$\frac{1}{3\cdot(\Pi_0+\pi_t^{(0)})}$; 4^2	
	κ_1	Coupling strength to π_1	0.05 ; 0			
	ω_1	Learning rate of π_1	0.1 ; 4^2		$\log\left(\frac{1}{\hat{\pi}_1^{(0)}} - \frac{1}{\pi_1^{(0)}}\right)$; 0	
	$\mu_2^{(0)}$	Initial mean of 2^{nd} level	0 ; 0			
	$\sigma_2^{(0)}$	Initial variance of 2^{nd} level	3 ; 4^2			3 ; 4^2
	ϑ_2	Learning rate of π_1	-8 ; 0		$\frac{1}{\hat{\pi}_2^{(0)}} - \frac{1}{\pi_2^{(0)}}$; 0	
	m_1	Restriction parameter	- ; -	- ; -	0.5; 0	
			Model 1	Model 2	Model 3	Model 4
Tinnitus Precursor	$\mu_t^{(0)}$	Mean of tinnitus precursor	- ; -	- ; -	$\mu_1^{(0)} \cdot (0.5 \cdot (\sqrt{\frac{u_s}{\mu_1^{(0)}}} - 1) + 1)$; 4^2	
	κ_t	Coupling strength to π_t	- ; -	- ; -	- ; -	0.05 ; 0
	ω_t	Learning rate of π_t	- ; -	- ; -	$\log\left(\frac{\mu_t^{(0)}\cdot\left(\mu_1^{(0)}-\mu_t^{(0)}\right)^2}{\mu_p - 0.5\cdot\mu_1^{(0)}}\right)$; 0	
	$b^{(0)}$	Initial mean of 2^{nd} level	- ; -	- ; -	- ; -	0 ; 0
	$\sigma_b^{(0)}$	Initial variance of 2^{nd} level	- ; -	- ; -	- ; -	5 ; 4^2
	ϑ_b	Learning rate of π_b	- ; -	- ; -	- ; -	$\frac{1}{\hat{\pi}_b^{(0)}} - \frac{1}{\pi_b^{(0)}}$; 0
	m_b	Restriction parameter	- ; -	- ; -	- ; -	5 ;4^2
Response Model			Model 1	Model 2		
	ζ	Inverse decision	0.001 ; 4^2	0.001 ; 0		

prior distribution of the model parameters and optimised with a quasi-Newton optimisation algorithm. For model inversion (model fitting), the HGF-Toolbox version 4.1 from the TAPAS package was used (Toolbox, 2020). To validate the performance of the tHGF the protected exceedance probability (PXP) using the log model evidence (LME) was calculated for each of the 8 models. The LME metric considers the trade-off between model architecture and model fit by penalizing model complexity. Across all subjects, the PXP showed that the full tHGF with the subject-specific noise parameter for the response model (PXP = 0.97) explained the

behavior of the subjects with the highest probability. Therefore, the reproduction of RI and additional simulations were performed with the full tHGF and the subject-specific response model.

2.4 Model Test Scenarios

To assess the generality of the tHGF, three scenarios of common perceptual tinnitus phenomena were simulated with the identical model structure: 1) residual inhibition, 2) residual excitation and 3) the occurrence of tinnitus in non-tinnitus subjects after temporary sensory deprivation (e.g. as caused by ear plugs or a longer stay in a soundproof chamber). For all simulations, the model input (i.e. the external stimulus in dB SL) was used to generate the model output (i.e. the behavioral responses indicating tinnitus loudness mapped to dB SL).

2.4.1 Residual Inhibition

Testing of the RI scenario was performed by applying the subject-specific parameters found from model inversion to the model using the same subject-specific acoustic stimulation to generate the behavioral responses in our cohort. We compared the generated model output with the raw data of each subject's behavioral response with the aim of reducing possible information added by pre-processing. Data at the same time points after auditory stimulation as the raw data were sampled from the generated model output over ten trials. A linear regression with zero intercept was performed for each subject using the raw data as the dependent variable and the sampled model output as the independent variable. The linear correlation coefficient was used to assess the similarity of the model output with

the subject responses. In order to investigate the influence of the coupling factor κ_t, which controls the volatility of beliefs in the tinnitus precursor, on RI, the model outputs were additionally evaluated using six empirically selected magnitudes for the tinnitus precursor coupling factor ($\kappa_t = 0, 0.001, 0.005, 0.01, 0.05, 0.1$). As a saturation of RI even using extended stimulation durations was observed by Terry et al. (1983), we compared the model output with four stimulation durations (5, 10, 60, and 180 seconds) to evaluate RI saturation effects predicted by the model.

2.4.2 Residual Excitation

Sedley et al. (2016a) suggested that stimulation at a level similar to that of the tinnitus precursor could lead the brain to believe it will perceive a higher intensity by modifying the default prior and/or posterior to become more similar to the tinnitus precursor, resulting in a temporary enhancement in tinnitus perception while reducing the precision-weighted prediction error (PWPE). To investigate whether the tHGF model could replicate this phenomenon with the same model structures (i.e., fitted values of model parameter using RI behavioral data), we applied the stimulation at a level identical to the estimated mean of the tinnitus precursor to simulate RE for an exemplary subject in the second scenario (i.e. $u_s \stackrel{!}{=} U_t$).

2.4.3 Transition from Residual Inhibition to Residual Excitation

Since we assume that perceptually similar stimuli can produce RE, a transition of the effect from weak RI to RE and back to RI should be observed for increasing stimulation levels, depending on the tinnitus precursor. Furthermore, it was shown that higher intensities produce stronger RI (Terry et al., 1983). To illustrate

the transition, we computed and compared the synthetic output of the tHGF for different stimulation levels.

2.4.4 Tinnitus after Temporary Sensory Deprivation

An empirical study reported 64% of subjects without tinnitus experienced tinnitus-like sounds after sitting in a sound booth for 20 minutes (Tucker et al., 2005). Another study demonstrated that 70% of participants wearing a monaural earplug experienced tinnitus on the plugged side (17/27 in the plugged ear only, or in both ears, but louder in the plugged ear 2/27) (Brotherton et al., 2019). Accordingly, it was hypothesized that the occurrence of tinnitus in subjects without tinnitus after a prolonged stay in a silent environment (e.g., in an acoustic chamber or with the use of earplugs) would cause an increase in the sensitivity of sensory cells in the deprived regions potentially leading to an increase in neural response gain in the central auditory system (Hullfish et al., 2019b, Schaette et al., 2012). This can be modelled by an decreased restriction parameter (m_b) of the auto-regressive process in the second level of the tinnitus precursor. For the third scenario, a synthetic non-tinnitus subject was created by setting the initial parameter of the posterior perception to a small value ($\mu_1^{(0)} = 0.01$). The coupling factor was also set to a small value to mimic the minor volatility in the tinnitus precursor ($\kappa_t = 0.001$). The initial values of the other model parameters were updated according to Table 1. Sensory deprivation was simulated by manually modulating the value of m_b for the subject (without changing other model parameters). Additionally, we hypothesized that non-tinnitus subjects experiencing no tinnitus after staying in a silent environment (around 30 % (Brotherton et al., 2019)) might have minimal tinnitus precursor volatility. To test this assumption, a second synthetic non-tinnitus subject was

329 created with $\kappa_t = 0.0001$.

3 Results

3.1 Residual inhibition

Figure 3 (a) and (b) illustrate the model parameter trajectories of the tHGF levels for an exemplary subject (subject number 22). Figure 3 (a) shows a rapid decrease in the precision-weighted prediction error of the tinnitus precursor at stimulus onset and a gradual decrease during stimulation. In the absence of external acoustic stimulation, the error increases again to reach the previous level. Consequently, the uncertainty of the tinnitus precursor increases during stimulation, but returns to its initial state after stimulus offset (yellow shaded area in Figure 3 (b)). The large tinnitus precursor uncertainty leads to a temporary reduction of the perceived tinnitus level immediately after the stimulus, eventually converging toward the initial tinnitus level (blue line in Figure 3 (a)), which corresponds to a typical RI response. Supplementary Table S2 summarizes the fitted values of the model parameter.

3.1.1 Influence of Coupling Factors

The trajectories of the posterior of the second level of the tinnitus precursor (i.e. μ_b) reflect the evolution of its precision (i.e. π_t), which is influenced by the coupling factor κ_t. Figure 3 (c) and (d) illustrate the impact of different magnitudes of κ_t on RI and the tinnitus level. Increased values of κ_t accelerate the decrease of the tinnitus precursor's precision to reach saturation during stimulation (upper panel of Figure 3 (c)), allowing maximum suppression of the tinnitus perception after stimulation offset. However, they also increase the recovery of the tinnitus (i.e. less time of suppression). Low values of κ_t reduce the influence of the

acoustic stimulation on the precision leading to a partial suppression of the tinnitus ($\kappa_t = 0.001$) or no suppression at all ($\kappa_t = 0$).

3.1.2 Influence of Stimulus Duration

Figure 4 compares the RI responses for four different stimulation durations. With a sufficiently long acoustic stimulation (60 seconds), the uncertainty of the tinnitus precursor reaches the saturation level (Figure 4 (a)), resulting in maximum tinnitus suppression (Figure 4 (b)). An prolonged stimulation duration (180 seconds) does not further increase the uncertainty of the tinnitus precursor. The trajectories of the uncertainty of the tinnitus precursor and the posterior perception μ_1 after stimulation offset (right panels of Figure 4 (a) and (b)) are nearly identical for the 60 and 180 seconds stimuli. In contrast, an insufficient stimulation length (5 seconds and 10 seconds) results in a smaller tinnitus precursor uncertainty, which indicates a stronger belief in the tinnitus precursor and leads to less tinnitus suppression (Figure 4).

3.1.3 Comparison with Raw Data

We observed a median linear regression coefficient of 0.79 for all 46 subjects in Figure 5, indicating that the generative model is able to reproduce the behavioral responses of the subjects in most of the cases.

3.2 Residual excitation

The tHGF was able to reproduce RE with the trained model parameters in all subjects (RE duration; median: 152 seconds; inter-quartile range: 91 seconds). The

simulation of RE on an exemplary subject is illustrated in Figure 6. A stimulation at a level equal to the mean value of the individual tinnitus precursor ($u_s = U_t$) leads to an increase in the precision of the tinnitus precursor. This causes a stronger belief in the tinnitus precursor, resulting in a perceived tinnitus loudness at the level of the tinnitus precursor, which is per definition higher than the initial tinnitus loudness level. Therefore, an enhancement of the tinnitus loudness can be observed after stimulation offset. The tinnitus loudness level returns to its original level after approximately 30 seconds after the stimulation offset in the exemplary subject. Similar to the RI scenario, the stimulation results in a decrease of precision-weighted prediction errors for the tinnitus precursor, which return to pre-stimulation levels over time.

The simulation of the different behavioral responses of an exemplary subject (subject 26) after a range of stimulation levels from low to high is demonstrated in Figure 7. The transition from a weak RI effect at a low stimulation level, to RE using levels similar to the tinnitus precursor, back to RI can be observed. An RI effect can be observed for stimulation levels deviating from the level of the tinnitus precursor. The opposite is observed when the stimulation level is close to the tinnitus precursor, resulting in RE with a maximum effect when stimulated exactly at the tinnitus precursor.

3.3 Tinnitus after Temporary Sensory Deprivation

The simulated behavioral response for the synthetic non-tinnitus subject ($\kappa_t = 0.001$) is shown in Figure 8. In the first 250 seconds the subject perceives silence due to the low precision of the tinnitus precursor. Between 250 and 1200 seconds,

the restriction parameter for the second level of the tinnitus precursor (m_b) is reduced to mimic deprived sensory cells caused by earplugs or a silent environment. This causes the precision of the tinnitus precursor to increase (i.e. a decrease in the yellow shaded areas in the lower panel of Figure 8). Over time, the the non-tinnitus subject is perceiving the tinnitus. After resetting the parameter m_b, (i.e. the earplugs are removed or the subject leaves the acoustic chamber) the tinnitus gradually disappears. Figure 9 shows the behavioral responses for the second synthetic non-tinnitus subject with minimal tinnitus precursor volatility (i.e. $\kappa_t = 0.0001$). No tinnitus could be perceived in this subject.

4 Discussion

This study presents the tHGF, a Bayesian generative computational model that enables to estimate the behavioral response of tinnitus subjects in experiments involving acoustic stimulation. The applicability of the model was demonstrated in three common perceptual tinnitus phenomena: RI, RE, and occurrence of tinnitus after sensory deprivation.

4.1 Residual Inhibition and Residual Excitation

Sedley et al. (2016a) introduced the term "tinnitus precursor" to describe the sensory input that corresponds to the spontaneous activity along the auditory pathway. They suggested that a bottom-up compensation could be reflected as a modulation of the tinnitus precursor. Furthermore, resetting the default silence prediction could be considered as a maladaptive top-down compensation. Increasing the precision of the tinnitus precursor (with an inherently low precision in non-tinnitus cases) would lead to the occurrence of tinnitus, while shifting the mean value of the default silence prediction to a certain intensity would contribute to the development of chronic tinnitus. Temporary tinnitus suppression following acoustic stimulation (i.e. RI) could be understood as a decrease in the precision or intensity of the tinnitus precursor. Presentation of a stimulus that is perceptually similar to the tinnitus precursor would lead to a shift of the prediction distribution towards the tinnitus precursor or a decrease of the prediction precision, resulting in a stronger belief in the perception of tinnitus at a higher intensity (i.e. RE). Both phenomena, RI and RE, would result in a decrease in precision-weighted prediction errors. Since the amplitude of gamma oscillations in the auditory cortex has been

assumed to reflect precision-weighted prediction errors (Sedley et al., 2016a), the approach explains the paradox of reduced gamma oscillations in both RI and RE.

For the RI scenario, the overall acceptable correlation between the model-generated and measured behavioral responses demonstrates the applicability of the tHGF model. Roberts et al. (2008) suggested that RI corresponds to a temporal re-balancing of neural excitation and inhibition after the presentation of a stimulus with sufficient intensity, which manifests as a decrease in neuronal synchronicity in deafferent regions.

Since the tinnitus precursor represents a sensory input, we argue that reducing its precision relatively limits the excitatory influence on the auditory cortex and thus could be considered as restoring the balance of excitation and inhibition. Furthermore, hearing loss could lead to an increase in the sensitivity of cells in deafferented regions to detect the missing information (Hullfish et al., 2019b). According to our model, this is reflected in the increase in the precision of the tinnitus precursor. With sufficient stimulation the sensitivity is temporarily downgraded leading to RI. In addition, low frequency neural oscillations have been discussed as being responsible for modulating the precision of the tinnitus precursor. The decrease in precision in tHGF can be interpreted as the observed decrease in low frequency oscillations in the auditory cortex during RI in the human neuronal imaging studies (Adjamian et al., 2012, Kahlbrock and Weisz, 2008, Sedley et al., 2012, 2015), while the decrease in gamma oscillations could be interpreted as a minimization of precision-weighted prediction errors of the tinnitus precursor as mentioned above. Alternatively, RI could be explained by forward masking of spontaneous activity in the auditory pathway, which would reduce the intensity of the tinnitus precursor instead of its precision (Sedley et al., 2016a).

In the RE scenario, stimulation of the subject's individual fitted tinnitus precursor resulted in increased precision of the tinnitus precursor, which would lead to a stronger belief of the subject in the tinnitus precursor. Since the tinnitus precursor (obtained through model fitting) has a higher intensity than the original tinnitus loudness, both prediction and posterior perception would update towards a higher perceptual intensity hence a higher tinnitus perception after acoustic stimulation. Similar to the RI scenario, the model reproduces reduced precision-weighted prediction errors of the tinnitus precursor during stimulation. The reduced prediction errors can be interpreted as a reduction in gamma oscillations, as observed in previous tinnitus studies for both RI and RE (Arnal et al., 2011, Sedley et al., 2016b). Considering the successful generation of synthetic behavioral responses after acoustic stimulation that reflected the RE phenomenon in all subjects in our cohort, it is worth discussing whether all tinnitus subjects could experience RE through a specific stimulus at their tinnitus precursor that is of higher intensity than the tinnitus loudness. In previous studies, RE was observed in the minority (from a range of about 7-27%) subjects (Neff et al., 2019, Sedley et al., 2012). According to the tHGF model, one explanation for the occurrence of RE in a limited number of subjects could be the coincidental use of an acoustic stimulation level close to the individuals' tinnitus precursor.

The transition of behavioral responses using different levels of stimulation also suggests that no change in tinnitus perception, RI, and RE might be experienced by the same subject. In our case, a stimulation level close to that of the tinnitus precursor produces an enhancement of the tinnitus for a subject who experienced RI when using a sufficiently high stimulation level, or no change in perception when simulating with a level not similar to the tinnitus precursor (below or above

the tinnitus precursor). Future work to investigate this speculation, not only considering the similarity in stimulation level but also spectral characteristics, is worth to be performed. In line with the literature (Terry et al., 1983), Figure 7 also illustrates the transition from low RI effect to a substantial RI effect when sweeping from low to high stimulation levels.

4.2 Tinnitus Precursor Coupling Factor

In our model, the suppression effect (i.e. the depth and duration of RI) is influenced by the coupling factor of the tinnitus precursor. The uncertainties (i.e., inverse precision) of the tinnitus precursor increase logarithmically to saturation to prevent them from becoming infinite, while the growth rate depends positively on the coupling factors κ_t. Therefore, we argue that the volatility of individuals' belief in the perception of tinnitus, which depends on the external environment, is controlled by a certain strength κ_t. The less confident a subject is about the tinnitus precursor, the stronger their belief in the perception of silence after the stimulation will be. A full suppression of tinnitus can only be achieved by saturation of the uncertainty of the tinnitus precursor. Lower coupling factors κ_t result in an overall lower RI depth (i.e. less suppression). In the extreme case of $\kappa_t = 0$, the subject perceives the tinnitus at the previous level immediately after the stimulation offset. In other words, these subjects experience neither tinnitus suppression nor enhancement. Conversely, larger coupling factors, i.e. the strength of volatility to the change in the external environment, also lead to a faster recovery of uncertainty, resulting in a shorter RI time. Interestingly, in our previous work we observed a slightly increased maximal suppression effect immediately after the stimulation offset, but a

modestly shortened RI time after ten consecutive RI assessments (Hu et al., 2021). In combination with tHGF, this might be explained by a minor increase in coupling factors after ten repetitions of RI.

The coupling parameters control the volatility of beliefs in the tinnitus precursor. Partyka et al. (2019) have postulated that the predisposition to developing tinnitus may be contingent on an individual's tendency to engage in auditory predictive processing (i.e. strength of reliance on pre-existing beliefs). Here, the proposition is that individuals with tinnitus exhibited stronger expectations which in turn induce the pre-activation of tonotopically specific stimulus templates in the auditory cortex in order to pre-empt expected inputs. This notion has some neurobiological plausibility since, in the visual cortex, it has been shown that expectations induce similar patterns of cortical activation compared to the actual visual stimulus (Kok et al., 2017).

4.3 Stimulation Duration

Using the tHGF, we demonstrated that the RI depth and duration saturate with increased stimulus durations as the precision of the tinnitus precursor saturates. This is in accordance to the work of Terry et al. (1983), who observed a non-linear saturation effect. Further studies, with refined stimulation protocols need to be performed to test the predictions of the tHGF model.

4.4 Tinnitus Occurrence in Non-tinnitus Subjects

The occurrence of tinnitus in non-tinnitus individuals is a common phenomenon. According to current tinnitus model proposed by Sedley et al. (2016a), non-tinnitus

subjects have a tinnitus precursor with a relatively high uncertainty. In a previous study, auditory phantom sensation could be induced in the majority of subjects after placing them in a sound-proven booth within 20 minutes (Tucker et al., 2005). Similarly, the majority of subjects who used earplugs experienced a phantom sound (Brotherton et al., 2019, Schaette et al., 2012). This phenomenon may be explained by an increase in neural gain, based on the theory of gain adaptation and/or homeostatic plasticity in response to auditory deprivation. The increased neural gain in turn may be reflected as an increased bottom-up sensory expectation or an increased tinnitus precursor precision for Bayesian brain-based tinnitus theories. In the case of the tHGF, the neuronal changes in the auditory system might be accounted by the model parameters at the higher levels of the tinnitus precursor. Therefore, we expected the occurrence of tinnitus in non-tinnitus subjects after adjusting the values of model parameters in the second level of the tinnitus precursor, that mimic the consequences of sensory deprivation, e.g., gain adaptation mechanism and homeostatic plasticity. In this study, we have demonstrated that the tHGF enables the reversible occurrence of tinnitus by modulation of the restriction parameter m_b, which functions to prevent the subject from infinitely increasing the belief of perceiving an intensity as the tinnitus precursor. The decreased m_b could reflect gain adaptation or homeostatic plasticity and allows the synthetic subject to increase the belief in the tinnitus precursor, resulting in an increase in auditory perception. After resetting m_b to the original value, the synthetic subject's perception returns to silence, which is consistent with a previous study in which earplugs were used to produce a tinnitus-like perception that disappeared after the earplugs were removed (Schaette et al., 2012). Furthermore, the tinnitus was not perceived by the synthetic subject with minimal tinnitus precursor volatility. The

different results due to individual model parameters could provide an explanation for the subgroup without tinnitus after staying in a silent environment.

4.5 Prediction of Residual Excitation Stimulation

The model provides the opportunity to quantitatively test the speculation of the experience of RE in individuals with RI. Based on the tinnitus loudness, stimulation level, and the behavioral response of a subject, a stimulation level that can produce RE (i.e., at the fitted level of the tinnitus precursor) could be estimated. A study paradigm including this hypothesis could provide strong evidence for or against the basic assumptions underlying our model.

4.6 Strengths and Limitations

The tHGF demonstrates the potential of computational modeling and may provide new insights into tinnitus research. We believe that the use of computational modeling can bridge the gap between current tinnitus theories and behavioral and physiological observations by enabling the quantitative investigation of the proposed hypotheses. The assumption that insignificant and inconsistent results in the literature due to multiple synergistic mechanisms of tinnitus could be verified with a computational and empirically tested model has been proposed (Sedley, 2019). In addition, the model could be used as a basis for model development in future studies with refined behavioral tasks. Another capability of the model is the inference of its latent variables with behavioral and physiological states of the subjects after input stimuli. Combined with the estimation of individual model parameters for each subject, the model has the potential to guide specific treatment

outcomes for the individual.

One limitation of our study is the lack of evidence to associate the latent model parameters with physiological characteristics of the subjects. The RI test paradigm applied in this study (Hu et al., 2019) does not provide sufficient behavioral data to estimate the full range of model parameters or trajectories in the latent states that might enable an interpretation of physiological parameters. Therefore, the fitted model may be challenged with an overestimation of the parameters that may have reached local minima during optimization. Further model-optimized tasks, e.g. performing RI with different stimulation levels and durations or tasks suitable for measuring mismatch negativity (MMN), are required in future studies to validate and advance the model. Furthermore, the presented model does not include the entire range of tinnitus-related psychoacoustic features. The model could be further advanced by including other factors such as tinnitus laterality and spectral information.

Another limitation of our work is that the behavioral responses used for model fitting applied a sigmoid function mapped from the original discrete responses from a Likert scale of ten trials. The preprocessing the raw data could introduce additional information that would contaminate the model fit. This was performed due to the small amount of sparsely sampled data and the potential inherent uncertainties of the subjects in behavioral decisions. Future studies could either apply behavioral test paradigms with continuous responses or directly use binary (Mathys et al., 2014) or categorical levels with a higher sampling rate as model input (i.e. without preprocessing) for fitting. Furthermore, although we used LME to account for the model complexity and model fit, the paradigm of using a single stimulation level in this work may not provide enough observations to cover the

full range of the data distribution, leading to possible overfitting and the potential problem of local minima. Future experiments with different stimulation levels that provide additional information complementing the necessary observations would improve the goodness of fit. Also, responses with more time stamps would provide more information that would enable the development of a more sophisticated response model for estimating subject-specific behavior. In this study only a single group of tinnitus subjects with RI was included, and no neuroimaging analysis was performed. The combination of computer modeling, functional neuroimaging and clinical measures could further extend the model and enable model-based neuroimaging analyses such as fMRI and EEG/MEG. A correlation between model parameters and trajectories of hidden states with neuronal activity in specific regions in the auditory system and other part of the brain of different subgroups (i.e. with the control group) would consolidate the model and provide evidence for the role of the Bayesian brain in tinnitus physiology. Nevertheless, the presented work is part of an ongoing study involving within-subject EEG measurements in combination with repeatable RI. The collected EEG data will be analysed together with tHGF. Further details on the measurement procedure are available in (Hu et al., 2019). Beside the bottom-up compensation in the auditory system, previous studies showed that other non-auditory systems, including memory, attention and limbic systems, can be involved in the development and maintenance of tinnitus (De Ridder et al., 2014b, 2015, Rauschecker et al., 2015, Roberts et al., 2013). The necessity of establishing a default tinnitus prediction has been suggested to cause chronic tinnitus (Sedley et al., 2016a). To simplify the model, the development of tinnitus chronification was not included in the tHGF. Nevertheless, the precision of $u_s = 0$ (i.e. Π_0) can be used to model the belief in the perception of silence.

Modulation of Π_0 can therefore represent a shift of the default prediction from silence toward tinnitus.

In future work, the model can be extended to include modulation of top-down and bottom-up mechanisms to describe the development of tinnitus. For instance, an additional component can be introduced that is automatically updated over time in response to the external and internal environment to control for maladaptive top-down compensation and thus the default tinnitus prediction. It can be speculated that the updating of this component is related to the failure of noise cancellation from the frontostrial gating model and modifications in the salience and memory network. Furthermore, its changes in responses to sensory input can provide predictions for restoring the default prediction of silence. In addition, the model may include a component related to hearing impairment that automatically modifies the model parameters of the tinnitus precursor to reflect the consequence of sensory deprivation, e.g. gain adaption, homeostatic or allostatic plasticity. Alternatively, other tinnitus-related computational models that focus on the microscopic level can be used to link to the specific model parameters (Schaette and Kempter, 2012).

5 Conclusion

We present a computational model based on the Bayesian brain framework to quantitatively and qualitatively explain perceptual tinnitus phenomena. The replication of RI as well as the simulation of other common perceptual tinnitus phenomena demonstrates the applicability of the model to capture processes involved in tinnitus. Our approach introduces generative computational modeling to the research field of tinnitus. It has the potential to quantitatively link experimental observations to

644 theoretical hypotheses and to support the search for neural signatures of tinnitus
645 by finding correlates between the latent variables of the model and measured
646 physiological data, and consequently to predict the outcomes of specific treatments
647 for individuals.

648 Funding

649 This study was in part supported by the Purma foundation, the Dunemere founda-
650 tion, the Béatrice Ederer-Weber foundation and the Wolfermann-Nägli foundation.

651 Competing interest

652 The authors declare no conflict of interest.

Supplementary material

Table S1: Overview of demographic details, tinnitus characteristics and residual inhibition outcomes of 46 subjects with substantial residual inhibition (RI depth ≤ -4) and RI time less than 5 minutes. HL = hearing level; PTA = pure-tone average over 0.5, 1, 2, 4 and 8 kHz; THI = tinnitus handicap inventory; HADS = hospital anxiety and depression scale; SL = sensation level. Continuous variables are summarized with their mean values (± standard deviation).

	RI (n=46)
Gender	
Female	16 (35%)
Male	30 (65%)
Age, years	49.3 (±13.3)
Hearing threshold at tinnitus pitch, dB HL	40.0 (±25.6)
Hearing threshold (PTA), dB HL	15.5 (±13.6)
Tinnitus chronicity, years	9.84 (±10.1)
Tinnitus form	
Noise-like	8 (17%)
Pure-tone	38 (83%)
Tinnitus laterality	
Bilateral	20 (43%)
Central	9 (20%)
Unilateral	17 (37%)
Tinnitus pitch, kHz	8.7 (±3.1)
Tinnitus loudness, dB SL	0.3 (±7.5)
Minimum masking level, dB SL	16.9 (±12.5)
Loudness discomfort level, dB SL	46.0 (±15.5)
THI score	28.0 (±20.3)
HADS-A score	5.3 (±3.1)
HADS-D score	3.8 (±3.4)
Averaged maximum RI depth	-4.7 (±0.3)
Averaged maximum RI time, seconds	93.3 (±49.4)

Table S2: Summary of fitted parameter values of tHGF. Fixed parameters vary between subjects.

	Parameter	Description	Mean (min - max)	Fixed / Fitted
Model Input/Output				
Sensory Stimulation	u_s	Stimulation level (dB SL)	35.77 (17 - 69.50)	Fixed
	Π_s	Precision with stimulation	1.38 (0.01 - 8.12)	Fitted
	Π_0	Precision without stimulation	48.03 (1.94 - 436.44)	Fixed
Responses	y	Auditory perception (dB SL)	N/A	N/A
Perceptual Model				
Perception	$\mu_1^{(0)}$	Initial mean of inferred perception	6.54 (1 - 36.5)	Fixed
	$\sigma_1^{(0)}$	Initial variance of μ_1	5.68 (0.52 - 26.31)	Fitted
	κ_1	Coupling strength to π_1	0.05	Fixed
	ω_1	Learning rate of π_1	2.53 (-1.35 - 6.25)	Fixed
	$\mu_2^{(0)}$	Initial mean of 2^{nd} level	0	Fixed
	$\sigma_2^{(0)}$	Initial variance of 2^{nd} level	17.14 (0.29 - 140.05)	Fitted
	ϑ_2	Learning rate of π_1	0.23 ($3 * 10^{-5}$ - 3.61)	Fixed
	m_1	Restriction parameter	0.5	Fixed
Tinnitus Precursor	$\mu_t^{(0)}$	Mean of tinnitus precursor	9.05 (1.32 - 43.43)	Fitted
	κ_t	Coupling strength to π_t	0.05	Fixed
	ω_t	Learning rate of π_t	2.19 (-0.19 - 4.42)	Fixed
	$b^{(0)}$	Initial mean of 2^{nd} level	0	Fixed
	$\sigma_b^{(0)}$	Initial variance of 2^{nd} level	4.97 (1.42 - 14.86)	Fitted
	ϑ_b	Learning rate of π_b	0.04 (0.02 - 0.27)	Fixed
	m_b	Restriction parameter	4.93 (0.97 - 10.76)	Fitted
Response Model	ζ	Inverse decision	0.06 ($2 * 10^{-4}$ - 0.77)	Fitted

References

Adjamian, P., Sereda, M., Zobay, O., Hall, D. A., and Palmer, A. R. Neuromagnetic indicators of tinnitus and tinnitus masking in patients with and without hearing loss. *Journal of the Association for Research in Otolaryngology*, 13(5):715–731, 2012.

Arnal, L. H., Wyart, V., and Giraud, A.-L. Transitions in neural oscillations reflect prediction errors generated in audiovisual speech. *Nature neuroscience*, 14(6):797, 2011.

Brotherton, H., Turtle, C., Plack, C. J., Munro, K. J., and Schaette, R. Earplug-induced changes in acoustic reflex thresholds suggest that increased subcortical neural gain may be necessary but not sufficient for the occurrence of tinnitus. *Neuroscience*, 407:192–199, 2019.

Carpenter-Thompson, J. R., Akrofi, K., Schmidt, S. A., Dolcos, F., and Husain, F. T. Alterations of the emotional processing system may underlie preserved rapid reaction time in tinnitus. *Brain research*, 1567:28–41, 2014.

Cassidy, C. M., Balsam, P. D., Weinstein, J. J., Rosengard, R. J., Slifstein, M., Daw, N. D., Abi-Dargham, A., and Horga, G. A perceptual inference mechanism for hallucinations linked to striatal dopamine. *Current Biology*, 28(4):503–514, 2018.

Chrostowski, M., Yang, L., Wilson, H. R., Bruce, I. C., and Becker, S. Can homeostatic plasticity in deafferented primary auditory cortex lead to travelling waves of excitation? *Journal of computational neuroscience*, 30(2):279–299, 2011.

Clark, A. Whatever next? predictive brains, situated agents, and the future of cognitive science. *Behavioral and brain sciences*, 36(3):181–204, 2013.

Corlett, P. R., Horga, G., Fletcher, P. C., Alderson-Day, B., Schmack, K., and Powers III, A. R. Hallucinations and strong priors. *Trends in cognitive sciences*, 23(2):114–127, 2019.

De Ridder, D., Elgoyhen, A. B., Romo, R., and Langguth, B. Phantom percepts: tinnitus and pain as persisting aversive memory networks. *Proceedings of the National Academy of Sciences*, 108(20):8075–8080, 2011.

De Ridder, D., Joos, K., and Vanneste, S. The enigma of the tinnitus-free dream state in a bayesian world. *Neural Plasticity*, 2014, 2014a.

De Ridder, D., Vanneste, S., and Freeman, W. The bayesian brain: phantom percepts resolve sensory uncertainty. *Neuroscience & Biobehavioral Reviews*, 44:4–15, 2014b.

De Ridder, D., Vanneste, S., Weisz, N., Londero, A., Schlee, W., Elgoyhen, A. B., and Langguth, B. An integrative model of auditory phantom perception: tinnitus as a unified percept of interacting separable subnetworks. *Neuroscience & Biobehavioral Reviews*, 44:16–32, 2014c.

De Ridder, D., Vanneste, S., Langguth, B., and Llinas, R. Thalamocortical dysrhythmia: a theoretical update in tinnitus. *Frontiers in neurology*, 6:124, 2015.

Eggermont, J. J. and Roberts, L. E. The neuroscience of tinnitus. *Trends in neurosciences*, 27 (11):676–682, 2004.

Fournier, P., Cuvillier, A.-F., Gallego, S., Paolino, F., Paolino, M., Quemar, A., Londero, A., and Norena, A. A new method for assessing masking and residual inhibition of tinnitus. *Trends in hearing*, 22:2331216518769996, 2018.

Friston, K. The free-energy principle: a unified brain theory? *Nature reviews neuroscience*, 11(2): 127–138, 2010.

Galazyuk, A., Voytenko, S., and Longenecker, R. Long-lasting forward suppression of spontaneous firing in auditory neurons: Implication to the residual inhibition of tinnitus. *Journal of the Association for Research in Otolaryngology*, 18(2):343–353, 2017.

Gault, R., McGinnity, T. M., and Coleman, S. Perceptual modeling of tinnitus pitch and loudness. *IEEE Transactions on Cognitive and Developmental Systems*, 12(2):332–343, 2020.

Güntensperger, D., Thüring, C., Meyer, M., Neff, P., and Kleinjung, T. Neurofeedback for tinnitus treatment – review and current concepts. *Frontiers in Aging Neuroscience*, 9:386, 2017. ISSN 1663-4365. doi: 10.3389/fnagi.2017.00386. URL `https://www.frontiersin.org/article/10.3389/fnagi.2017.00386`.

Hu, S., Anschuetz, L., Huth, M. E., Sznitman, R., Blaser, D., Kompis, M., Hall, D. A., Caversaccio, M., and Wimmer, W. Association between residual inhibition and neural activity in patients with tinnitus: Protocol for a controlled within-and between-subject comparison study. *JMIR research protocols*, 8(1):e12270, 2019.

Hu, S., Anschuetz, L., Hall, D. A., Caversaccio, M., and Wimmer, W. Susceptibility to residual inhibition is associated with hearing loss and tinnitus chronicity. *Trends in Hearing*, 25: 2331216520986303, 2021.

Hullfish, J., Abenes, I., Kovacs, S., Sunaert, S., De Ridder, D., and Vanneste, S. Functional brain changes in auditory phantom perception evoked by different stimulus frequencies. *Neuroscience letters*, 683:160–167, 2018.

Hullfish, J., Abenes, I., Yoo, H. B., De Ridder, D., and Vanneste, S. Frontostriatal network dysfunction as a domain-general mechanism underlying phantom perception. *Human brain mapping*, 40(7):2241–2251, 2019a.

Hullfish, J., Sedley, W., and Vanneste, S. Prediction and perception: Insights for (and from) tinnitus. *Neuroscience & Biobehavioral Reviews*, 102:1–12, 2019b.

Jastreboff, P. J. Phantom auditory perception (tinnitus): mechanisms of generation and perception. *Neuroscience research*, 8(4):221–254, 1990.

Kahlbrock, N. and Weisz, N. Transient reduction of tinnitus intensity is marked by concomitant reductions of delta band power. *BMC Biology*, 6(1):4, 2008.

Knill, D. C. and Pouget, A. The bayesian brain: the role of uncertainty in neural coding and computation. *TRENDS in Neurosciences*, 27(12):712–719, 2004.

Kok, P., Mostert, P., and De Lange, F. P. Prior expectations induce prestimulus sensory templates. *Proceedings of the National Academy of Sciences*, 114(39):10473–10478, 2017.

Kumar, S., Sedley, W., Barnes, G. R., Teki, S., Friston, K. J., and Griffiths, T. D. A brain basis for musical hallucinations. *Cortex*, 52:86–97, 2014.

729 Lee, S.-Y., Nam, D. W., Koo, J.-W., De Ridder, D., Vanneste, S., and Song, J.-J. No auditory
730 experience, no tinnitus: lessons from subjects with congenital-and acquired single-sided deafness.
731 *Hearing Research*, 354:9–15, 2017.

732 Mathys, C., Daunizeau, J., Friston, K. J., and Stephan, K. E. A bayesian foundation for individual
733 learning under uncertainty. *Frontiers in human neuroscience*, 5:39, 2011.

734 Mathys, C. D., Lomakina, E. I., Daunizeau, J., Iglesias, S., Brodersen, K. H., Friston, K. J., and
735 Stephan, K. E. Uncertainty in perception and the hierarchical gaussian filter. *Frontiers in*
736 *human neuroscience*, 8:825, 2014.

737 McCormack, A., Edmondson-Jones, M., Somerset, S., and Hall, D. A systematic review of the
738 reporting of tinnitus prevalence and severity. *Hearing research*, 337:70–79, 2016.

739 Neff, P., Zielonka, L., Meyer, M., Langguth, B., Schecklmann, M., and Schlee, W. Comparison
740 of amplitude modulated sounds and pure tones at the tinnitus frequency: residual tinnitus
741 suppression and stimulus evaluation. *Trends in hearing*, 23:2331216519833841, 2019.

742 Norena, A. and Eggermont, J. Changes in spontaneous neural activity immediately after an
743 acoustic trauma: implications for neural correlates of tinnitus. *Hearing research*, 183(1-2):
744 137–153, 2003.

745 Noreña, A. J. and Eggermont, J. J. Enriched acoustic environment after noise trauma abolishes
746 neural signs of tinnitus. *Neuroreport*, 17(6):559–563, 2006.

747 Norena, A. J. An integrative model of tinnitus based on a central gain controlling neural sensitivity.
748 *Neuroscience & Biobehavioral Reviews*, 35(5):1089–1109, 2011.

749 Parra, L. C. and Pearlmutter, B. A. Illusory percepts from auditory adaptation. *The Journal of*
750 *the Acoustical Society of America*, 121(3):1632–1641, 2007.

751 Partyka, M., Demarchi, G., Roesch, S., Suess, N., Sedley, W., Schlee, W., and Weisz, N. Phantom
752 auditory perception (tinnitus) is characterised by stronger anticipatory auditory predictions.
753 *bioRxiv*, page 869842, 2019.

Powers, A. R., Mathys, C., and Corlett, P. Pavlovian conditioning–induced hallucinations result from overweighting of perceptual priors. *Science*, 357(6351):596–600, 2017.

Rao, R. P. and Ballard, D. H. Predictive coding in the visual cortex: a functional interpretation of some extra-classical receptive-field effects. *Nature neuroscience*, 2(1):79–87, 1999.

Rauschecker, J. P., May, E. S., Maudoux, A., and Ploner, M. Frontostriatal gating of tinnitus and chronic pain. *Trends in cognitive sciences*, 19(10):567–578, 2015.

Roberts, L. E., Moffat, G., Baumann, M., Ward, L. M., and Bosnyak, D. J. Residual inhibition functions overlap tinnitus spectra and the region of auditory threshold shift. *Journal of the Association for Research in Otolaryngology*, 9(4):417–435, 2008.

Roberts, L. E., Husain, F. T., and Eggermont, J. J. Role of attention in the generation and modulation of tinnitus. *Neuroscience & Biobehavioral Reviews*, 37(8):1754–1773, 2013.

Schaette, R. and Kempter, R. Development of tinnitus-related neuronal hyperactivity through homeostatic plasticity after hearing loss: a computational model. *European Journal of Neuroscience*, 23(11):3124–3138, 2006.

Schaette, R. and Kempter, R. Predicting tinnitus pitch from patients' audiograms with a computational model for the development of neuronal hyperactivity. *Journal of neurophysiology*, 101(6):3042–3052, 2009.

Schaette, R. and Kempter, R. Computational models of neurophysiological correlates of tinnitus. *Frontiers in systems neuroscience*, 6:34, 2012.

Schaette, R. and McAlpine, D. Tinnitus with a normal audiogram: physiological evidence for hidden hearing loss and computational model. *Journal of Neuroscience*, 31(38):13452–13457, 2011.

Schaette, R., Turtle, C., and Munro, K. J. Reversible induction of phantom auditory sensations through simulated unilateral hearing loss. *PLoS One*, 7(6):e35238, 2012.

Sedley, W. Tinnitus: does gain explain? *Neuroscience*, 407:213–228, 2019.

779 Sedley, W., Teki, S., Kumar, S., Barnes, G. R., Bamiou, D.-E., and Griffiths, T. D. Single-subject
780 oscillatory gamma responses in tinnitus. *Brain*, 135(10):3089–3100, 2012.

781 Sedley, W., Gander, P. E., Kumar, S., Oya, H., Kovach, C. K., Nourski, K. V., Kawasaki, H.,
782 Howard III, M. A., and Griffiths, T. D. Intracranial mapping of a cortical tinnitus system
783 using residual inhibition. *Current Biology*, 25(9):1208–1214, 2015.

784 Sedley, W., Friston, K. J., Gander, P. E., Kumar, S., and Griffiths, T. D. An integrative tinnitus
785 model based on sensory precision. *Trends in Neurosciences*, 39(12):799–812, 2016a.

786 Sedley, W., Gander, P. E., Kumar, S., Kovach, C. K., Oya, H., Kawasaki, H., Howard III, M. A.,
787 and Griffiths, T. D. Neural signatures of perceptual inference. *Elife*, 5:e11476, 2016b.

788 Sedley, W., Alter, K., Gander, P. E., Berger, J., and Griffiths, T. D. Exposing pathological
789 sensory predictions in tinnitus using auditory intensity deviant evoked responses. *Journal of*
790 *Neuroscience*, 39(50):10096–10103, 2019.

791 Seki, S. and Eggermont, J. J. Changes in spontaneous firing rate and neural synchrony in cat
792 primary auditory cortex after localized tone-induced hearing loss. *Hearing research*, 180(1-2):
793 28–38, 2003.

794 Silchenko, A. N., Adamchic, I., Hauptmann, C., and Tass, P. A. Impact of acoustic coordi-
795 nated reset neuromodulation on effective connectivity in a neural network of phantom sound.
796 *Neuroimage*, 77:133–147, 2013.

797 Stephan, K. E., Iglesias, S., Heinzle, J., and Diaconescu, A. O. Translational perspectives for
798 computational neuroimaging. *Neuron*, 87(4):716–732, 2015.

799 Terry, A., Jones, D., Davis, B., and Slater, R. Parametric studies of tinnitus masking and residual
800 inhibition. *British journal of audiology*, 17(4):245–256, 1983.

801 Toolbox, T. https://translationalneuromodeling.github.io/tapas, 2020.

802 Tucker, D. A., Phillips, S. L., Ruth, R. A., Clayton, W. A., Royster, E., and Todd, A. D. The
803 effect of silence on tinnitus perception. *Otolaryngology—Head and Neck Surgery*, 132(1):20–24,
804 2005.

805 Vanneste, S. and De Ridder, D. Deafferentation-based pathophysiological differences in phantom
806 sound: tinnitus with and without hearing loss. *Neuroimage*, 129:80–94, 2016.

807 Xiong, B., Liu, Z., Liu, Q., Peng, Y., Wu, H., Lin, Y., Zhao, X., and Sun, W. Missed hearing loss
808 in tinnitus patients with normal audiograms. *Hearing research*, 384:107826, 2019.

809 Zeng, F.-G. An active loudness model suggesting tinnitus as increased central noise and hyperacusis
810 as increased nonlinear gain. *Hearing Research*, 295:172–179, 2013.

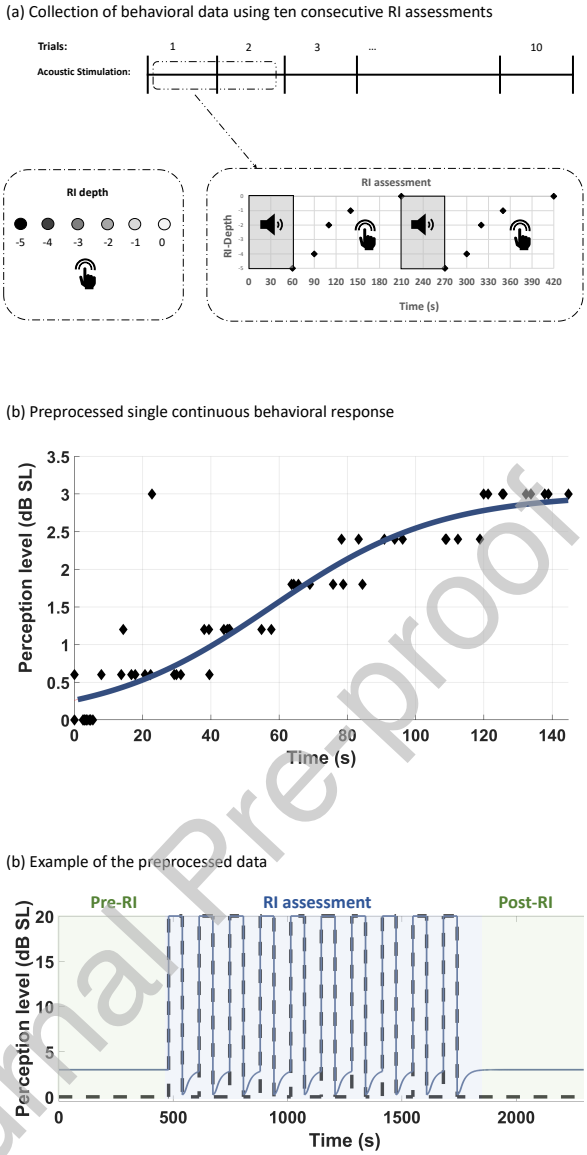

Figure 2: **(a)** Behavioral data collection using ten consecutive trials with acoustic stimulation of 60 seconds duration. After stimulus offset, the subjects were asked to indicate the residual inhibition (RI) depth on a Likert scale. Consecutive trials were initiated after the subjects indicated the return of the tinnitus to the initial loudness level. **(b)** The categorical behavioral responses collected during the residual inhibition task were mapped to continuous dB sensation level (SL) values and fitted with a sigmoid function to produce a single continuous trajectory for each subject. The black diamonds represent the combined behavioral responses of ten trials, while the blue line indicates the fitted trajectory. **(c)** To generate the model output, the fitted trajectory was replicated ten times, interleaved by the acoustic stimulation. In addition, eight-minute non-stimulus periods before and after the assessment task were added (green areas). The black dashed line represents the model input with 0 dB SL for silence and a subject-specific level (here: 20 dB SL) for acoustic stimulation. The blue solid line represents the model output reflecting the auditory perception.

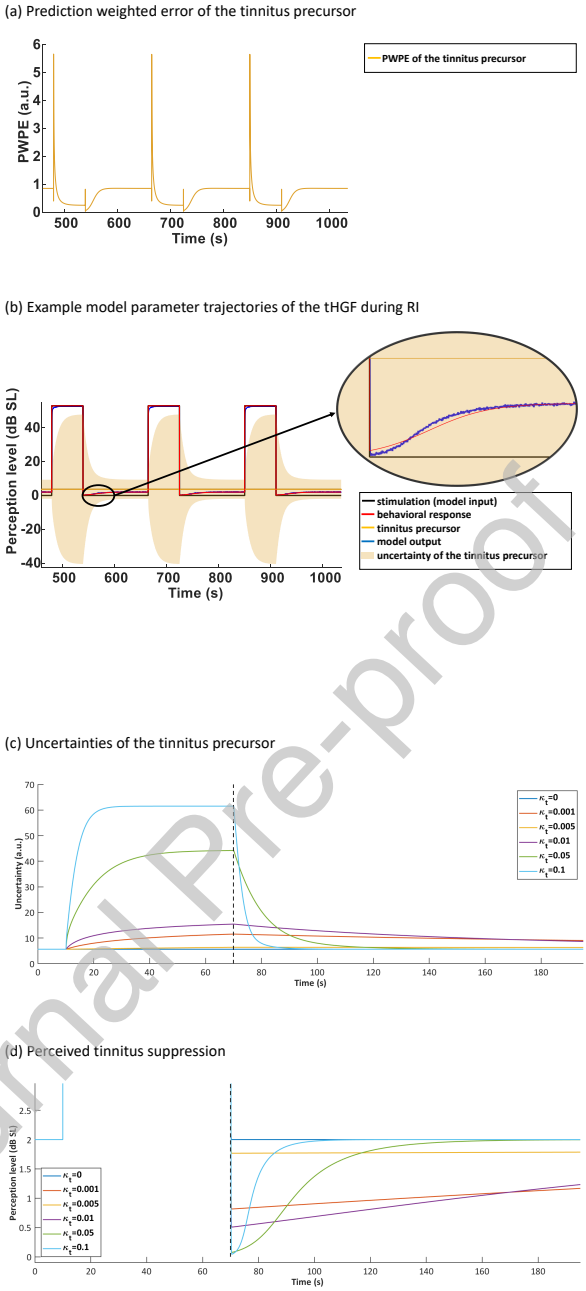

Figure 3: Panels **(a)** and **(b)** demonstrate the trajectories of the tHGF during residual inhibition shown for three out of ten repetitions. **(a)** Precision-weighted prediction error (PWPE) of the tinnitus precursor. **(b)** Acoustic stimulation level (model input; black line), mapped behavioral response of the subject (red line), tinnitus precursor (yellow line) and the simulated behavioral response from the tHGF model (model output; blue line). The yellow shaded area represents the uncertainty (95% confidence interval) of the tinnitus precursor. Panels **(c)** and **(d)** show the effect of the coupling factor κ_t demonstrated in a single trial with a 60-second stimulus with 53 dB SL. The black dotted line represents the stimulus offset. The uncertainties of the tinnitus precursor are shown in **(c)**. The trajectories in **(d)** represent the auditory perception (posterior μ_1).

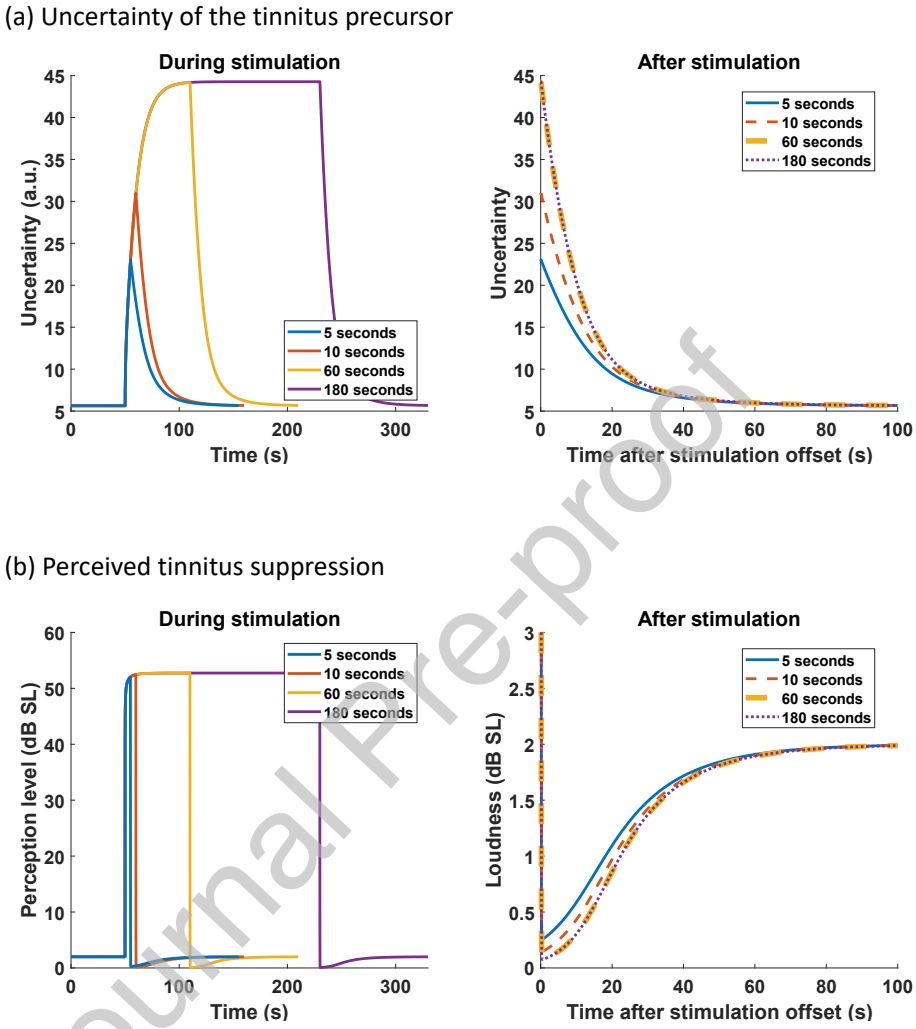

Figure 4: RI during stimulation (left hand side; solid lines) and after stimulation (right hand side; solid and dashed lines) for stimuli presented at 53 dB SL: Panel **(a)** shows the tinnitus precursor uncertainty for stimulus durations: 5 seconds (blue), 10 seconds (red), 60 seconds (yellow) and 180 seconds (purple). Panel **(b)** shows the perceived tinnitus suppression (i.e., posterior μ_1) of the four different stimulation durations.

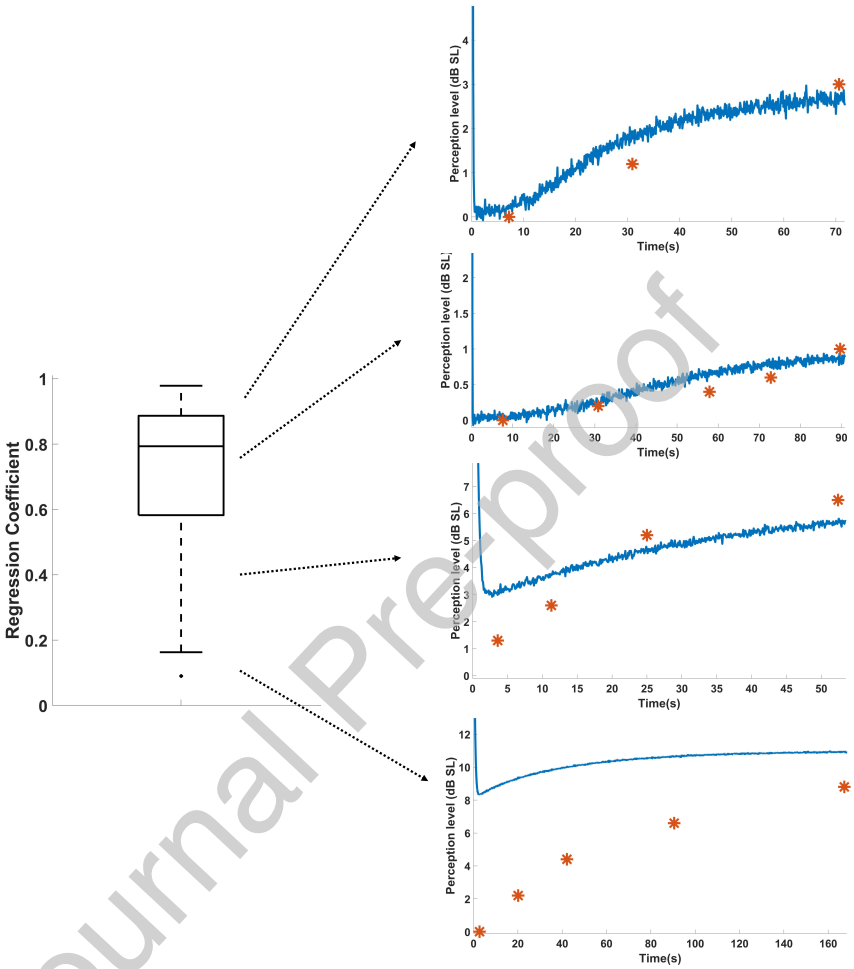

Figure 5: Linear regression coefficient between the tHGF model output and the behavioral responses of 46 tinnitus subjects. Example trajectories are shown for very low (0.16), low (0.42), medium (0.78) and high (0.95) linear regression coefficients. Red points indicate the raw behavioral responses and blue lines indicate the output of the tHGF model.

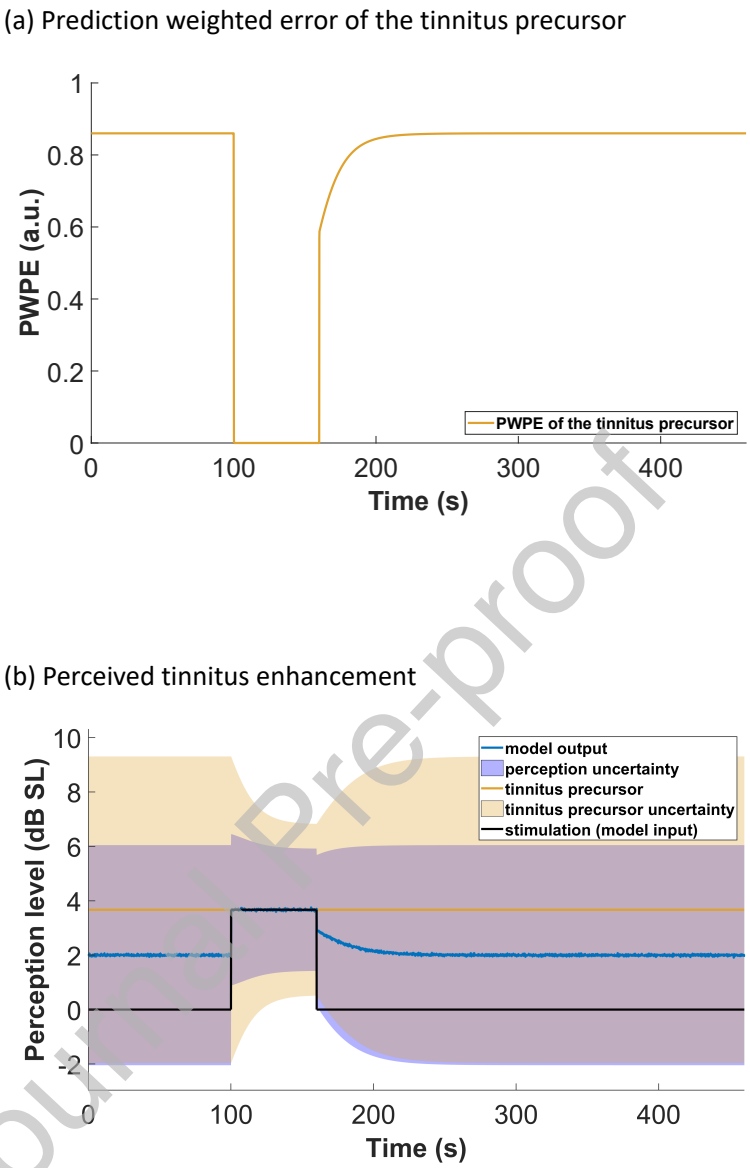

Figure 6: Trajectories of the tHGF in a simulated case of residual excitation. **(a)** Precision-weighted prediction error (PWPE) of the tinnitus precursor. **(b)** Acoustic stimulation level (model input, black line), simulated behavioral response of the subject (model output, blue line) and the tinnitus precursor (yellow line). In the RE scenario, the stimulation is presented at the mean value of the tinnitus precursor. The yellow and blue shaded areas represent the uncertainty (95% confidence interval) of the tinnitus precursor and the posterior, respectively.

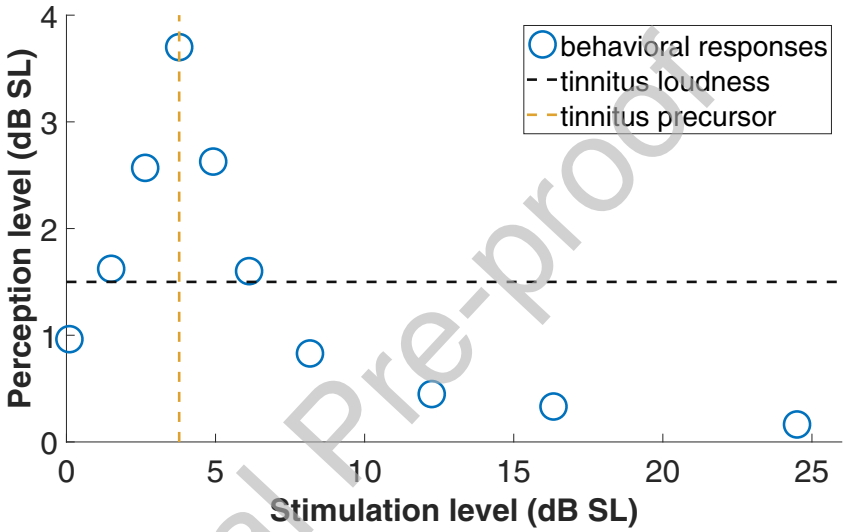

Figure 7: Behavioral response of an exemplary subject for different stimulation levels two seconds after stimulus offset, illustrating the predicted transition from a weak RI effect to RE and to strong RI, eventually saturating for high stimulation levels.

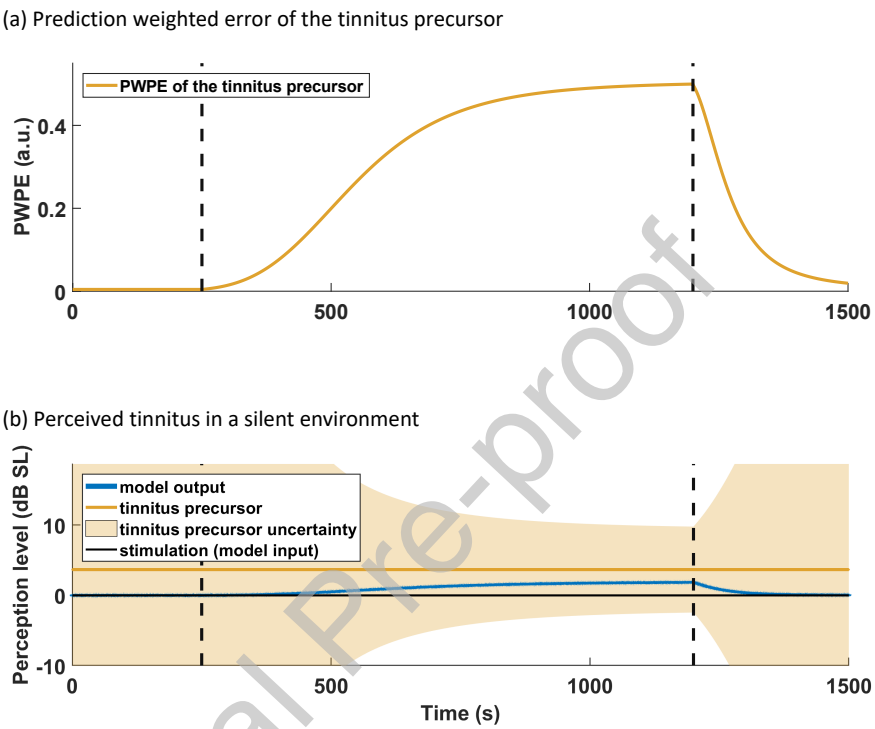

Figure 8: Simulated behavioral data of a synthetic non-tinnitus subject ($\kappa_t = 0.001$). **(a)** Precision-weighted prediction error (PWPE) of the tinnitus precursor. **(b)** Zero acoustic stimulation level (model input, black line), simulated behavioral response of the subject (model output, blue line) and the tinnitus precursor (yellow line). The yellow shaded area represents the uncertainty (95% confidence interval) of the tinnitus precursor. The black dotted lines represent the modification times of the model parameter. The synthetic subject perceives the tinnitus in the period between 250 and 1200 seconds.

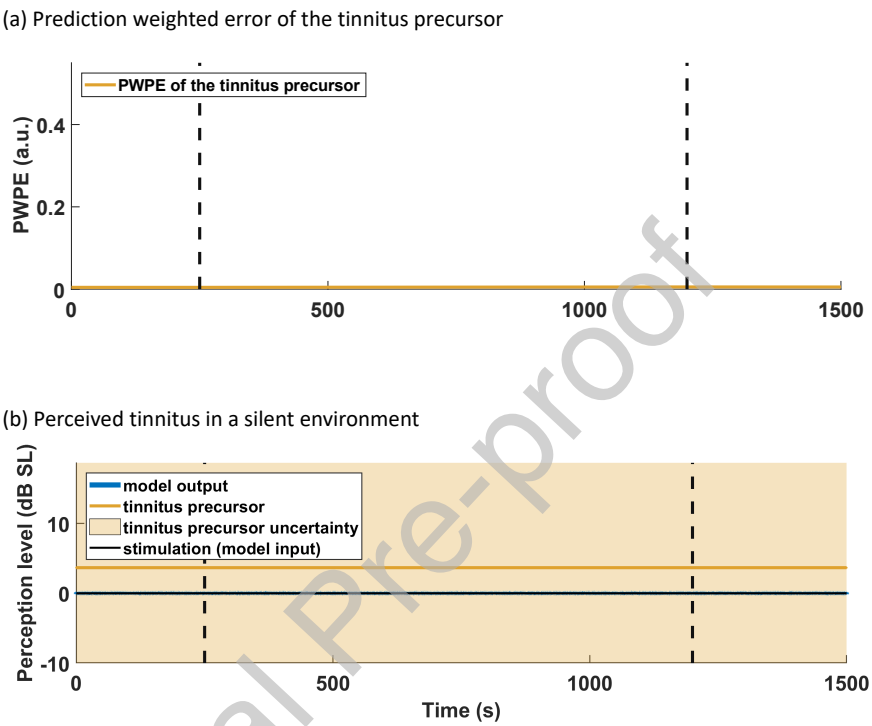

Figure 9: Simulated behavioral data of a synthetic non-tinnitus subject with minimal tinnitus precursor volatility (i.e. $\kappa_t = 0.0001$). **(a)** Precision-weighted prediction error (PWPE) of the tinnitus precursor. **(b)** Zero acoustic stimulation level (model input, black line), simulated behavioral response of the subject (model output, blue line), and the tinnitus precursor (yellow line). The yellow shaded area represents the uncertainty (95% confidence interval) of the tinnitus precursor. The black dotted lines represent the modification times of the model parameter. In this case, no tinnitus is perceived by the synthetic subject.

811

UNIVERSITÄT BERN

ARTORG CENTER
BIOMEDICAL ENGINEERING RESEARCH

INSELSPITAL

ARTORG Center for Biomedical Engineering Research, Murtenstrasse 50, CH-3008 Bern

Barbara Canlon, PhD
Editor-in-Chief
Hearing Research

Bern, February 22nd 2021

Declaration of interests

The authors declare that they have no known competing financial interests or personal relationships that could have appeared to influence the work reported in this paper.

Kind regards,

Dr. Wilhelm Wimmer

Tel: +41 (0)31 632 8789
Fax: +41 (0)31 632 7624
wilhelm.wimmer@artorg.unibe.ch
www.artorg.unibe.ch